ALL OPTICAL SENSORS USING SPECTRAL SWITCHING

A thesis submitted in partial fulfillment of the requirements for the award of degree of

Master of Science

In

Physics

Submitted by:

AMANDEEP KAUR

Roll No. 301404002

Under the guidance of

DR. SOUMENDU JANA

Associate Professor

SPMS,

Thapar University, Patiala

School of Physics and Materials Science

Thapar University,

Patiala-147001, INDIA

I affectionately dedicate this thesis to my brother "Arshdeep".

Certificate

I hereby certify that the work which has been presented in this thesis entitled, "All optical sensors using spectral switching", submitted in the partial fulfillment of the requirements for the award of degree of Masters of Science in Physics at Thapar University, Patiala, is an authentic record of my own work carried out under the supervision of Dr. Soumendu Jana, Associate Professor, School of Physics and Material Science and refers other researcher's work which are duly listed in the reference section. The intellectual content of this thesis is the product of my own work, and contains no material which to a substantial extent has been accepted for the award of any other degree at this or any other educational institution, except where due acknowledgment is made in the thesis.

Amandeep Kaur

Date: 15 July '16

(Amandeep Kaur)

Roll number: 301404002

This is to certify that the above statement made by the candidate is correct and true to the best of my knowledge.

Soumendu Jana

DR. SOUMENDU JANA

Associate Professor

School of Physics and Material Science

Thapar University, Patiala

Dr. Manoj Kumar Sharma

Professor and Head

School of Physics and Material Science

Thapar University, Patiala.

Dr. S.S. Bhatia

Dean of Academic Affairs

Thapar University, Patiala.

Acknowledgement

I would like to express my profound gratitude to my supervisor **Dr. Soumendu Jana** for for his patience, motivation, and immense knowledge. He consistently allowed this research work to be my own and steered me in the right direction by patiently correcting my writing and supporting my research. I couldn't have imagined having a better advisor and mentor than him for my thesis.

I would like to thank **Dr. Manoj Kumar Sharma** for providing me with an excellent atmosphere and all the necessary facilities for my research. I am thankful and indebted to **Ms. Baldeep Kaur** and **Mr. Gurkirpal Singh Parmar**, Research Scholars for all the fun, the stimulating discussions, for sharing their experiences and timely guidance and encouragement extended to me. I take this opportunity to express gratitude to all of the Department faculty members of School of Physics and Material Sciences for their help and support.

I also thank my parents for the unceasing encouragement, spiritual support and attention throughout this venture that were necessary to complete this thesis.

Above all I render my gratitude to the Almighty who bestowed me with the strength, good health and the vision to walk on the path of truth.

Date: 15 July '16

Amandeep Kaur

Amandeep Kaur

CONTENTS

Chapter-1

1.1 Introduction **1**

1.2 Review on Spectral Switching **2**

1.3 Motivation **4**

1.4 Objectives **6**

1.5 Methodology **6**

1.5.1 Pulse Propagation Equation 9

1.5.2 Split Step Fourier Transformation Method 14

1.5.3 Far Field Power Spectrum

Chapter-2

2.1 Elements of Spectral Switching and fiber optic sensors **20**

2.1.1 Diffraction 20

2.1.2 Spectral Switching 22

2.1.2.1 On Axis spectral switching 22

2.1.2.2 Off Axis spectral switching 22

2.1.3 Non-Linear Optics 23

2.1.4 Fiber Optic Sensors 25

Chapter-3

3.1 Results and Discussions **29**

3.1.1 Improvement in response of fiber optic pH sensor by using spectral switching 29

3.1.2 Improvement in response of fiber optic relative humidity sensor by using spectral switching 35

3.2 Conclusion **40**

List of Figures **41**

References **43**

Appendices **45**

Abstract

Many fascinating phenomena like spectral switching, wave front dislocations occur in the domain of singular optics. The phenomenon of spectral switching has been investigated for linear medium using different input pulses. For the first time, nonlinear medium is used to explore the concept of spectral switching. The spectral switching and fiber optic sensors have been combined. The fiber optic sensors modulate the intensity of light due to the effect of change in pH of the external environment and the results have been used to investigate the dependency of the critical angle on the varying pH. Further the fiber optic relative humidity sensors shifts the dip wavelength of the input pulse and this result has been utilized to explore the behavior of the output when the shifting of the pulse due to spectral switching and the relative humidity is combined. The shift of the output thus found is significant which is can help to increase the sensitivity of the fiber optic sensors towards the minute environmental changes. The results found by this collaboration have tremendous applications in data communication, all- optical switching and distant space communications due to the increase in sensitivity towards the variations in external perturbations.

Chapter-1

1.1 Introduction

The wave is a disturbance in the medium. If there is no boundary in the medium, the wave will spread out. The ray of light will bend slightly at the edges as it passes through some boundary. This phenomenon is called diffraction. The diffracted light can produce fringes of bright or dark intensity. The diffraction of light was experimentally observed using the single slit experiment. The diffraction pattern produced consists of dark and bright fringes. The points of dark color have zero intensity. At these points the phase of the light remains undetermined. This observation lead to the emergence of an interesting branch called singular optics and such points are termed as singular points. Many fascinating phenomena e.g. spectral shifting, spectral switching, wave front dislocations were observed near the domain of singular points. Many theoretical works have been embarked upon to understand the concept of spectral switching. After getting diffracted, the light produces the bright and dark fringes and at the points of zero intensity, the switching of frequency occurs. Though it has been experimentally verified, it is still a developing branch of physics.

In 1960's, the invention of laser paved a new way to enhance the data communication systems. This advancement in transmission systems provoked the researchers to enhance the area of research using optical fibers. Thus many attempts were made to minimize the losses in the optical fibers. Soon it was explored that due to minimum loss, the change in phase, intensity, wavelength due to outer parameters could be sensed at a better level. Thus the technique of using optical fibers as sensors was looked upon by the researchers giving birth to the fiber optic sensors technology. If the aperture is drawn on the end of the fiber optic sensor, after diffraction through it, the spectral switching phenomena can be observed. The important concept introduced here is that as the properties of light gets modulated after passing through the aperture; the modulated effect can be seen on the spectral switching phenomenon. The pH sensors and relative humidity sensors have been used to detect the pH and RH as perturbations from the external environment and these parameters modulates the intensity of light. The concept

of spectral switching and fiber optic sensors has not been clubbed together yet. For the first time fiber optic sensors have been associated with the spectral switching phenomenon. This collaboration can provide better level of sensitivity.

1.2 Review on Spectral Switching

The overlapping of two waves leads to constructive or destructive interference. The destructive interference occurs where the light vanishes. At these zero intensity points, the phase cannot be determined i.e. the phase amplitude vanishes. Thus these points are termed as phase singularities or singular points and the branch related to study of these points is called singular optics. It is vast subject and imparts a wide platform to study optical vortices and wave front dislocations near the singular points [1-2]. Such spectral behavior is induced by the phenomenon of diffraction. This anomalous behavior of light due to optical singularities was experimentally investigated by Nye and berry and Wright. Many fascinating phenomena e.g. spectral shifting, spectral switching, wave front dislocations were observed near the domain of singular points [3]. These are the key aspects of the field of singular optics. Gbur, Visser and Wolf showed that a fully coherent and partially coherent light undergoes substantial change at phase singularities i.e. the spectral anomalies were observed [4-5]. Later the polychromatic light was also used for instigating the above phenomena [6].

In 2002, Gbur et.al explained the concept theoretically that when a spatially fully coherent beam is diffracted through an aperture, some spectral anomalies were observed near phase singularities [5]. Popescu et.al verified the same by demonstrating experimentally in the same year. He showed that these spectral changes are the typical feature of polychromatic field near these singular points [6]. Pu et.al unveiled that brisk spectral shifts may occur for partially coherent light i.e., spectral switching can be observed for the same and Kandpal et.al confirmed the above results experimentally. The light gets diffracted through an aperture at some specific dimensions and at these analytical lengths switching was observed [7]. Results of investigations emphasized above have lead to rejuvenation of interest in the field of spectral switching. The polarization singularities as well as the singularities created by the Lissajous states have also

been probed for two-color vector field [8]. Investigations have been carried out with various other beams e.g. the partially coherent Gaussian–Schell model beams were studied by Palma et. Al. The use of aperture lens for propagation of GSM beams revealed that the spectral switching depends on three parameters; the truncation parameter, coherence parameter and Fresnel number. If these system parameters are chosen as per convenience, the desired variation of position, number, and transition amplitude of the spectral switch can be achieved [9]-[10]. In 2000, Jixiong Pu and Shojiro Nemoto remarked the dependence of spectral switch positions and spectral switch performance on half-width at half-maximum of the original spectrum and the ratio of the central obstruction of the source. They used circular aperture to investigate the results related to spectral switches and spectral shifts in the diffraction of partially coherent light [11]. It was observed that when an aperture lens is illuminated by a multimode laser i.e Hermite Gaussian beams instead of a fundamental mode laser, the spectral switch can take place in the neighborhood of focus. The importance of aperture diffraction an the above mentioned system parameters was also observed [12].

Investigating further, Zhao Guang et,al revealed the effect of astigmatism on spectral switches of polychromatic Gaussian Schell-model beams. It was described that the spectral switch can also take place in a geometrical focal plane where the intensity minimum occurs in the neighborhood points. They concluded that the diffraction through aperture play an important role in altering the parameters affecting spectral switching [13]. In 2001, Liuzhan Pan and Baida Lü studied that the spectral switch effect can not only be studied for partially coherent light passing through an aperture, but also as an extension to Young's two-slit experiment using partially coherent light [14]. The ultra short pulses were also given prominence due to their time duration and high peak intensity characteristics. An analytical solution for ultra short light pulses was derived for diffraction by a circular symmetric aperture which revealed that the pulse broadens about axial points at the positions where the intensity approaches zero [15]. In 2003, the anomalous spectral behavior of diffracted chirped Gaussian pulses was illustrated. Along with the truncation parameter, two new parameters were found to affect the spectral behavior. These were chirp parameter and the pulse duration which altered the central frequency as well as

the spectral width of the pulse. The results were illustrated using numerical examples and an analytical approach for the near field spectrum of chirped Gaussian beams [16].

Later, the tunability of spectral switching was highlighted and several researches have been undertaken to investigate the behavior. The critical angle i.e. the angle at which the far field spectrum splits into two equal lines was found to depend on the cosh parameter. This provided an idea of controlling the switching by controlling the cosh parameter [17]. The applications of spectral switching in distant atmospheric optical communication links, coding decoding, data hiding and many other fields tremendous applications have provoked the researchers to make more advancements in the field of singular optics and spectral switching [18].

1.3 Motivation

Till now the major application of spectral switching was found in data all-optical switching, data processing and terrestrial and space communications. Also the switching speed has some limitations. This problem can be solved and spectral switching can be applied in wider field if one can use some dispersive nonlinear media. Mostly linear medium has been used in both sides of the aperture in order to observe spectral switching. But if the dispersive nonlinear medium is placed between the source and the aperture, due to variations in the intensity dependent refractive index of medium, and /or dispersion there will be a change in the spectral switching. This interesting possibility somehow gone unnoticed by researchers and consequently no attention was paid to investigate spectral switching using nonlinear dispersive media. Also change of some property in a linear media that influences intensity might control spectral switching. There haven't been such studies yet with spectral switching. Diffraction induced spectral switching is performed in air, which has negligible nonlinearity. Our current interest aims to use a nonlinear media in place of air and to find the change in spectral switching by changing the medium properties through which light will pass. Here we are placing an aperture at the end of a fiber optic pH sensor. The sensor will response to the variation of pH in the surrounding media. Since the aperture is attached at the end of the sensor, it will create

diffraction induced spectral switching. This in turn will magnify the action of the pH sensor. This is more fascinating than that of linear medium, because of the availability of many potential control parameters. The schematic of using fiber optic sensors along with the spectral switching is shown in the Fig. (1.1).

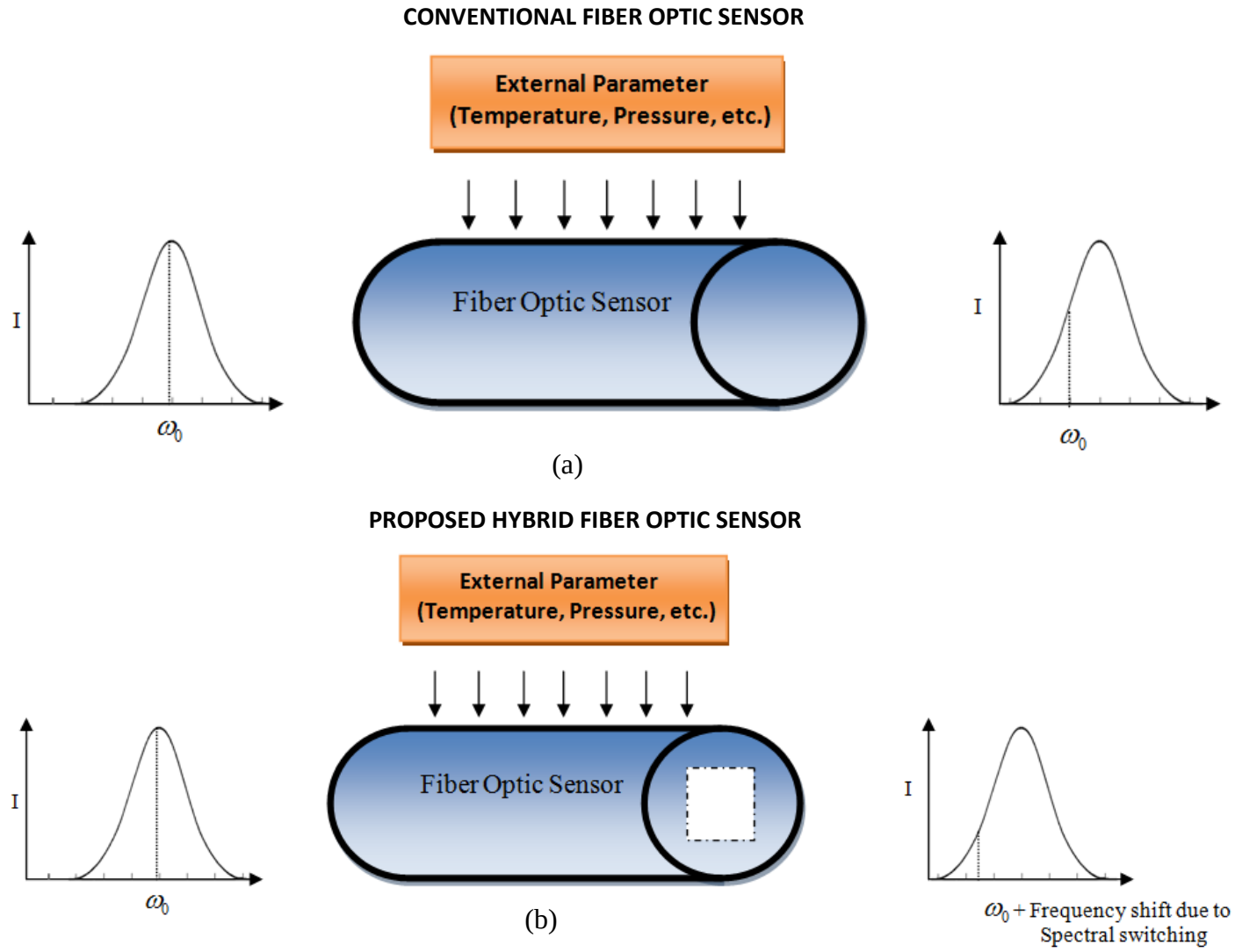

Figure 1.1 (a) The working of fiber optic sensors (b) the collaboration of fiber optic sensors and spectral switching to create hybrid sensors.

1.4 Objectives

The main objectives of the present investigation are as follows:

1. To study the response of a fiber optic pH sensor in conjugation with the spectral switching.
2. To improve the performance of a fiber optic relative humidity sensor by using the spectral switching.

1.5 Methodology

The strategy of the calculation we have done in the present investigation is as follows. As our thesis is aimed at using fiber optic sensors, the equation depicting the propagation of pulse through the fiber needs to be obtained. Therefore, in this section we derive the pulse propagation equation starting from the Maxwell's equations. Using SSFM we numerically obtain the pulse propagation through the fiber. The output will then be combined with the far field spectrum and further the numerical routine is carried out. Thus we have analytically derived the governing equation of pulse/beam diffraction including the aperture effects. We also show the basic of split step Fourier method.

The Maxwell equations form the basic foundation of the phenomena which involve electromagnetic components. These equations can offer a great help to study the propagation of optical fields in fibers. If H is the magnetic field vector and E is the electric field vector then, the Maxwell equations are written as [19]:

$$\nabla \times E = \partial B / \partial t, \tag{1.1}$$

$$\nabla \times H = J + \partial D / \partial t, \tag{1.2}$$

$$\nabla \cdot D = \rho_f, \tag{1.3}$$

$$\nabla \cdot B = 0, \tag{1.4}$$

B is the magnetic flux density, which is related to H by the relation $B = \mu_0 H$, where μ_0 is the vacuum permeability. Also D is the electric flux density which is related to E by the relation

$D = \varepsilon_0 E$, where ε_0 is the vacuum permittivity. By taking the bound charges and bound currents into account, new terms P and M are introduced which modify the above relations as:

$B = \mu_0 H$ +P where P is the polarization field, (1.5)

$D = \varepsilon_0 E$ +M where M is the magnetization field. (1.6)

The wave equations in terms of E and P can be obtained by taking the curl of the Maxwell's first Eq. (1.1) and substituting the values of other equations as well. The Eq. (1.1) thus gets reduced to the form:

$$\nabla \times \nabla \times E = -\frac{1}{c^2}\frac{\partial^2 E}{\partial t^2} - \mu_0 \frac{\partial^2 P}{\partial t^2}, \tag{1.7}$$

where, $c^2 = \frac{1}{\mu_0 \varepsilon_0}$ and c denotes the speed of light. To relate E and P and to find the value of P, quantum mechanical approach should be opted.

Here J is current density term and ρ_f depicts the charge density. When we suppose that the medium has no charge as well as current, these terms are considered equal to zero. To study the effect of electric field on bound charges, a general relation is introduced [20]-[23]:

$$P = \varepsilon_0 (\chi^{(1)} \cdot E + \chi^{(2)} : EE + \chi^{(3)} \vdots EEE + ...), \tag{1.8}$$

where, ε_0 is the vacuum permittivity. The terms $\chi^{(1)}$, $\chi^{(2)}, \chi^{(3)}$ and so on, are the first order, second order and third order susceptibility respectively. The first order linearity makes an effective contribution towards P by including the refractive index. The second order susceptibility basically involves the non-linear effects like second harmonic generation. For studying these effects, the wavelength varying from 0.5 to 2μm is of more interest. So by inclusion of the third order non-linear effect involving the term $\chi^{(3)}$, the polarization P splits into two parts,

$$P(r,t) = P_L(r,t) + P_{NL}(r,t) \ , \tag{1.9}$$

where $P_L(r,t)$ and $P_{NL}(r,t)$ includes the linear and non-linear terms. The electric field is related to P as follows [24]-]26] :

$$P_L(r,t) = \varepsilon_0 \int_{-\infty}^{\infty} \chi^{(1)}(t-t') \cdot E(r,t')dt', \tag{1.10}$$

$$P_{NL}(r,t) = \varepsilon_0 \int \int \int_{-\infty}^{\infty} \chi^{(3)}(t-t_1, t-t_2, t-t_3) \vdots \times E(r,t_1)E(r,t_2)E(r,t_3)dt_1 dt_2 dt_3 \tag{1.11}$$

The above mentioned equations present the general protocol to study the third order non-linear effects in optical fibers. It is generally considered that the nonlinear effects contribute very less to the induced polarization, so $P_{NL}(r,t)$ term is said to be the correction term. So we neglect this term and then the wave equation in terms of frequency domain is reduced to the form:

$$\nabla \times \nabla \times \tilde{E}(r,\omega) - \varepsilon(\omega)\frac{\omega^2}{c^2}\tilde{E}(r,\omega) = 0, \tag{1.12}$$

where $E(r,t)$ is reduced to the form $\tilde{E}(r,\omega)$ using Fourier Transformations and $\varepsilon(\omega)$ is the dielectric constant and it depends upon frequency, given by the relation:

$$\varepsilon(\omega) = 1 + \tilde{\chi}^{(1)}(\omega), \tag{1.13}$$

where $\tilde{\chi}^{(1)}(\omega)$ is obtained by reducing $\chi^{(1)}(t)$ into frequency domain. $\varepsilon(\omega)$ is a complex quantity, so we can split it into its real and imaginary parts. As the refractive index and absorption coefficient of the fiber depends on the frequency, the modified relation of dielectric constant is given by:

$$\varepsilon = \left(n + \frac{i\alpha c}{2\omega}\right)^2. \tag{1.14}$$

Here n and α are related to the linear susceptibility by the relations;

$$n(\omega) = 1 + \frac{1}{2}\,\mathrm{Re}\left[\tilde{\chi}^{(1)}(\omega)\right] \tag{1.15}$$

$$\alpha(\omega) = \frac{\omega}{nc}\,\mathrm{Im}\left[\tilde{\chi}^{(1)}(\omega)\right] \tag{1.16}$$

To simplify the Eq. (1.12), firstly we suppose that the loss in optical fibers is negligible and thus the imaginary part is neglected as compared to the real part. Hence following this concept, we replace $\varepsilon(\omega)$ by $\eta^2(\omega)$. Secondly, $\eta(\omega)$ does not depend on the properties of the core and the cladding, thus further we can simplify the Eq. (1.12) using the relation:

$$\nabla \times \nabla \times E \equiv \nabla(\nabla \cdot E) - \nabla^2 E = -\nabla^2 E, \tag{1.17}$$

where $\nabla \cdot D = 0 \Rightarrow \varepsilon(\nabla \cdot E) = 0$ (from Eq. (1.3)). Thus Eq. (1.12) is reduced to the form;

$$\nabla^2 \tilde{E} + n^2(\omega)\frac{\omega^2}{c^2}\tilde{E} = 0. \tag{1.18}$$

1.5.1 Pulse Propagation Equation

While studying the concept of nonlinear effects in optical fibers, we suppose that the width of the pulse varies between 10 ns to 10 fs. The shape and the spectrum of these short width pulses are affected by the dispersive properties of the media. From Eq. (1.9) and Eq. (1.17), the wave equation is expressed in the form:

$$\nabla^2 E - \frac{1}{c^2}\frac{\partial^2 E}{\partial t^2} = \mu_0\left[\frac{\partial^2 P_L}{\partial t^2} + \frac{\partial^2 P_{NL}}{\partial t^2}\right], \tag{1.19}$$

where P_L and P_{NL} are the linear and nonlinear parts of the induced polarization respectively.

Let us make some assumptions to simplify the above equation.

- The refractive index is not affected by the non-linear effects. Thus P_{NL} term is taken as a small disturbance and hence its effect is neglected.

- Though polarization maintaining fibers provide a better result, hence we must assume here that polarization remains conserved along the fiber.
- The optical field is supposed to be confined around a single frequency i.e. quasi-monochromatic where central frequency $\omega_0 \sim 10^{-15} s^{-1}$ and it is applicable to pulses with width similar to 0.1ps.

If we consider the case of slowly varying envelope approximation, the part of electric field $E(r,t)$ which varies quickly with time and space is written in the form:

$$E(r,t) = \frac{1}{2}\hat{x}\left[E(r,t)\exp(-i\omega_0 t) + c.c.\right], \tag{1.20}$$

Here, $\hat{x}$ is the polarization unit vector. The linear and nonlinear parts of the polarization can be represented in the same way as:

$$P_L(r,t) = \frac{1}{2}\hat{x}\left[P_L(r,t)\exp(-i\omega_0 t) + c.c.\right], \tag{1.21}$$

$$P_{NL}(r,t) = \frac{1}{2}\hat{x}\left[P_{NL}(r,t)\exp(-i\omega_0 t) + c.c.\right]. \tag{1.22}$$

Using the Eq. (1.21) in the Eq. (1.10), P_L is given by;

$$P_L(r,t) = \varepsilon_0 \int_{-\infty}^{\infty} \chi_{xx}^{(1)}(t-t')E(r,t')\exp\left[i\omega_0(t-t')\right]dt' \tag{1.23}$$

$$= \frac{\varepsilon_0}{2\pi}\int_{-\infty}^{\infty} \tilde{\chi}_{xx}^{(1)}(\omega)\tilde{E}(r,\omega-\omega_0)\exp\left[-i(\omega-\omega_{0)}t\right]d\omega, \tag{1.24}$$

where $E(r,t)$ is reduced to $\tilde{E}(r,\omega)$ using Fourier transformations.

Again using Eq. (1.22) in Eq. (1.11), and the time dependency of $\chi^{(3)}$ simplifies the equation by taking the nonlinear response to be instantaneous, $P_{NL}(r,t)$ is given by:

$$P_{NL}(r,t) = \varepsilon_0 \chi^{(3)} \vdots E(r,t)E(r,t)E(r,t) \tag{1.25}$$

Here we also assume that the molecular vibrations do not contribute to $\chi^{(3)}$ which is justified by Raman effect and the width of the pulse is estimated to be less than 1 ps. Using the Eq. (1.20) in Eq. (25), two terms are obtained. The first term oscillating at ω_0 is considered and the other term oscillating at higher frequency $3\omega_0$ is neglected in optical fibers. When Eq. (1.22) is substituted in Eq. (1.25), we obtain;

$$P_{NL}(r,t) \approx \varepsilon_0 \varepsilon_{NL} E(r,t), \tag{1.26}$$

where the dielectric constant in terms of nonlinearity is expressed as:

$$\varepsilon_{NL} = \frac{3}{4} \chi^3_{xxxx} \left| E(r,t) \right|^2. \tag{1.27}$$

$E(r,t)$ varies slowly with time and space, thus in order to obtain the wave equation, we use Fourier transformations. To achieve this approach, we suppose ε_{NL} to be constant [27]-[28]. Substituting Eqs. (1.20)- (1.22) in Eq. (1.19), the Fourier transformation of $E(r,t)$ into frequency domain is expressed as:

$$\tilde{E}(r, \omega - \omega_0) = \int_{-\infty}^{\infty} E(r,t) \exp\left[i(\omega - \omega_0)t \right] dt, \tag{1.28}$$

This satisfies the Helmholtz equation given by:

$$\nabla^2 \tilde{E} + \varepsilon(\omega) k_0^2 \tilde{E} = 0, \text{ where } k_0 = \omega / c, \tag{1.29}$$

and the dielectric constant in terms of nonlinearity is given by,

$$\varepsilon(\omega) = 1 + \tilde{\chi}^{(1)}_{xx}(\omega) + \varepsilon_{NL} \tag{1.30}$$

The refractive index and the absorption coefficient are used to define the nonlinear part of the dielectric constant and thus depend upon intensity. They can be defined as;

$$\tilde{n} = n + n_2|E|^2 \ , \qquad \tilde{\alpha} = \alpha + \alpha_2|E|^2 . \tag{1.31}$$

Thus using the above Eq. (1.31), the dielectric constant gets modified to the form;

$$\varepsilon = \left(\tilde{n} + \frac{i\tilde{\alpha}}{2k_0} \right)^2 . \tag{1.32}$$

Substituting the Eq. (1.32) and value of ε_{NL} from Eq. (1.27) the non-linear index n_2 and the two photon absorption coefficient α_2 of the fiber are expressed as:

$$n_2 = \frac{3}{8n}\mathrm{Re}(\chi^{(3)}_{xxxx}) \ , \qquad \alpha_2 = \frac{3\omega_0}{4nc}\mathrm{Im}((\chi^{(3)}_{xxxx}) \ . \tag{1.33}$$

The Helmholtz equation is solved using separation of variables. Let us suppose the solution of this equation is given by;

$$\tilde{E}(r, \omega - \omega_0) = F(x, y)\tilde{A}(z, \omega - \omega_0)\exp(i\beta_0 z) , \tag{1.34}$$

where $\tilde{A}(z, \omega)$ varies slowly with z and β_0 represents the wave number. Using the above solution, two equations obtained are of the form:

$$\frac{\partial^2 F}{\partial x^2} + \frac{\partial^2 F}{\partial y^2} + [\varepsilon(\omega)k_0^2 - \tilde{\beta}^2]F = 0 , \tag{1.35}$$

$$2i\beta_0 \frac{\partial \tilde{A}}{\partial z} + (\tilde{\beta}^2 - \beta_0^2)\tilde{A} = 0 . \tag{1.36}$$

The second order derivative of $\tilde{A}$ is ignored because it is considered that $\tilde{A}$ varies slowly with z. If Δn be the small perturbation, then the dielectric constant is reduced to the form:

$$\varepsilon = (n + \Delta n)^2 \approx n^2 + 2n\Delta n , \tag{1.37}$$

where,

$$\Delta n = n_2|E|^2 + \frac{i\tilde{\alpha}}{2k_0} . \tag{1.38}$$

Again here we replace ε by n^2 and the value of small perturbation Δn is included [29]. The modal distribution $F(x,y)$ is not influenced by Δn. The Eigen value is given by;

$$\tilde{\beta}(\omega) = \beta(\omega) = \Delta\beta\,, \tag{1.39}$$

Where

$$\Delta\beta = \frac{k_0 \int_{-\infty}^{\infty}\int \Delta n |F(x,y)|^2 \, dxdy}{\int_{-\infty}^{\infty}\int |F(x,y)|^2 \, dxdy}\,. \tag{1.40}$$

Thus the solution of the wave Eq. (1.19) in terms of first order perturbation is obtained. Again using the Eq. (1.20) and Eq. (1.34), the electric field is expressed as:

$$E(r,t) = \frac{1}{2}\hat{x}\{F(x,y)A(z,t)\exp[i(\beta_0 z - \omega_0 t)] + c.c.\}\,, \tag{1.41}$$

Here $A(z,t)$ is modified to $\tilde{A}(z,\omega-\omega_0)$ using the Fourier transform and then substituting the Eq. (1.36), we get

$$\frac{\partial\tilde{A}}{\partial z} = i[\beta(\omega) + \Delta\beta - \beta_0]\tilde{A}\,, \tag{1.42}$$

The above expression physically signifies the concept that a phase shift is experienced by each spectral component of the pulse during its propagation in the optical fiber. The phase shift depends on the intensity and frequency of the pulse.

In order to obtain the propagation equation in time domain, the inverse Fourier transformations can be applied to $\tilde{A}(z,\omega-\omega_0)$. By expanding $\beta(w)$ using Taylor series about ω_0,

$$\beta(\omega) = [\beta_0 + (\omega-\omega_0)\beta_1 + \frac{1}{2}(\omega-\omega_0)^2\beta_2 + \frac{1}{6}(\omega-\omega_0)^3\beta_3 + ...,] \tag{1.43}$$

Where

$$\beta_m = \left(d^m\beta / d\omega^m\right)_{\omega=\omega_0} \qquad (m = 1,2,...)\,.$$

If $\Delta\omega << \omega_0$, the higher order terms are neglected which also satisfies the assumption that the pulse has a defined central frequency. Thus using the expansion of $\beta(\omega)$ in Eq. (1.42) and then using the inverse Fourier transform, the equation becomes:

$$A(z,t) = \frac{1}{2\pi}\int_{-\infty}^{\infty} \tilde{A}(z,\omega-\omega_0)\exp[-i(\omega-\omega_0)t]d\omega. \tag{1.44}$$

$$\frac{\partial A}{\partial z} = -\beta_1\frac{\partial A}{\partial t} - \frac{i\beta_2}{2}\frac{\partial^2 A}{\partial t^2} + i\Delta\beta A, \tag{1.45}$$

where the differential operator $i\frac{\partial}{\partial t}$ is substituted instead of $\omega-\omega_0$ which is obtained by Fourier transform. Here the term $\Delta\beta$ accounts for the losses in fiber and the perturbation. By evaluating $\Delta\beta$ from the Eq. (1.38) and Eq. (1.40), and then substituting the value in Eq. (1.45), the final result obtained is:

$$\frac{\partial A}{\partial t} + \beta_1\frac{\partial A}{\partial t} + \frac{i\beta_2}{2}\frac{\partial^2 A}{\partial t^2} + \frac{\alpha}{2}A = i\gamma|A|^2 A, \tag{1.46}$$

where γ is the nonlinear parameter given by,

$$\gamma = \frac{n_2\omega_0}{cA_{eff}}.$$

1.5.2. Split Step Fourier Transformation Method

In order to understand the nonlinear effects in optical fibers, the analytical method generally makes the problem complex so we adopt the numerical approach. The numerical methods used can be distinguished into two categories: (1) Finite-Difference method; and (2) Pseudo-spectral method. The relative speed of Split Step Fourier Method (SSFM) is faster than other methods; hence this method is used to solve the pulse propagation equation in nonlinear dissipative medium. The methodology of SSFM is described as;

The NLS (Non-Linear Schrodinger) equation is written as:

$$\frac{\partial A}{\partial z} + i\frac{\beta_2}{2}\frac{\partial^2 A}{\partial t^2} - i\gamma|A|^2 A = 0, \tag{1.47}$$

$$\frac{\partial A}{\partial z} = \left[-i\frac{\beta_2}{2}\frac{\partial^2}{\partial t^2} + i\gamma|A|^2 A \right]. \tag{1.48}$$

The above Eq. (1.48) can be simplified as:

$$\frac{\partial A}{\partial z} = \left(\hat{D} + \hat{N}\right)A, \tag{1.49}$$

where $\hat{D} = -i\frac{\beta_2}{2}\frac{\partial^2}{\partial t^2}$ is the differential operator that includes the dispersion effects and the absorption as well as losses in the medium and $\hat{N} = i\gamma|A|^2$ is the nonlinear operator that determines the effect of fiber nonlinearities on pulse propagation. Generally, dispersion and non linearity act simultaneously along the fiber. We can achieve an approximate solution using SSFM. Here we suppose that while propagating over a small distance, the dispersion and non linearity act do not depend on each other and thus in more precise manner, propagation is done using h as the step size, from z to $z+h$. The two steps followed are

Step-1 Dispersive effects are ignored and only non linearity is taken into account i.e. $\hat{D} = 0$.

The Eq. (1.49) is reduced to the form:

$$\frac{\partial A}{\partial z} = \hat{N}A. \tag{1.50}$$

Integrating the above equation over the limits $A(z,t)$ to $A(z+h,t)$, we get

$$\int_{A(z,t)}^{A(z+h,t)} \frac{\partial A}{A} = \hat{N}\int_{z}^{z+h} \partial z \;\Rightarrow\; A(z+h,t) = A(z,t)\exp(h\hat{N}). \tag{1.51}$$

Step-2 The effect of fiber non linearities are ignored i.e. $\hat{N} = 0$

The Eq. (1.49) is reduced to the form

$$\frac{\partial A}{\partial z} = \hat{D}A. \tag{1.52}$$

Integrating the above equation over the limits $A(z,t)$ to $A(z+h,t)$, we get

$$\int_{A(z,t)}^{A(z+h,t)} \frac{\partial A}{A} = \hat{D}\int_{z}^{z+h} \partial z \;\Rightarrow\; A(z,t)\exp(h\hat{D}). \tag{1.53}$$

The solution obtained after combining the Step-1 and Step-2 is

$$A(z+h,t) \approx \exp(h\hat{D})\exp(h\hat{N})A(z,t). \tag{1.54}$$

If ω is the frequency, then the differential operator $\partial/\partial t$ is changed to $-i\omega$ in order to evaluate the operator $\exp(h\hat{D})$ using the Fourier transformation. Thus the value of differential operator including the dispersive effects gets modified to $\hat{D} = \frac{i\beta_2}{2}\omega^2$. Then operator $\exp(h\hat{D})$ can be expressed as:

$$\exp(h\hat{D})B(z,t) = F_T^{-1}\exp(h\hat{D}(-i\omega))F_T B(z,t). \tag{1.55}$$

Thus the explicit solution of the NLS equation is given by:

$$A(z+h,t) = \exp(h(\hat{D}+\hat{N}))A(z,t). \tag{1.56}$$

Baker-Hausdorff formula for two non-commuting operators $\hat{a}$ and $\hat{b}$ is given as:

$$\exp(\hat{a})\exp(\hat{b}) = \exp(\hat{a}+\hat{b}+\frac{1}{2}\left[\hat{a},\hat{b}\right]+\frac{1}{12}\left[\hat{a}-\hat{b},[\hat{a},\hat{b}]\right]+.....), \tag{1.57}$$

where $[\hat{a},\hat{b}] = \hat{a}\hat{b}-\hat{b}\hat{a}$. Taking $\hat{a} = h\hat{D}, \hat{b} = h\hat{N}$ along with Eq. (1.55), the factor $\frac{1}{2}h^2\left[\hat{D},\hat{N}\right]$ governs the prominent error term. Thus the split step Fourier method is found to be precise up to the 2nd order of the step size h. In order to further enhance the accuracy of SSFM, a different approach can be used. In this approach, the Eq. (1.54) is expressed as:

$$A(z+h,t)=\exp\left(\frac{h}{2}\hat{D}\right)\exp\left(\int_{z}^{z+h}\hat{N}(z')dz'\right)\exp\left(\frac{h}{2}\hat{D}\right)A(z,t). \qquad (1.58)$$

the exponential operators used in the above scheme are symmetric in nature, thus this approach is known as symmetric SSFM.[30] The middle term of the above expression shows the dependency of operator $\hat{N}$ on z.Thus this scheme depicts the concept that the non linearity acts at the center of the segment instead of acting on the boundary of the segment. If the value of step size h is presumed to be small, then the middle term gets reduced to the form $\exp(h\hat{N})$ which makes the Eq. (1.54) and Eq. (1.58) equal. This method is found to be more precise up to the third order of h and hence is more appropriate than the previous method. The accuracy of the SSF can be further achieved by integrating the middle integral part of the Eq. (1.58) by employing the trapezoidal rule as [31]:

$$\int_{z}^{z+h}\hat{N}(z')dz' \approx \frac{h}{2}\left[N(z)-\hat{N}(z+h)\right], \qquad (1.59)$$

The above expression is quite difficult to solve because the value of $\hat{N}(z+h)$ is not known at $z+\frac{h}{2}$. Thus in order to solve the above problem, the iterative method is followed. Here, the fiber length is divided into parts which may or may not be spaced equally. Then the optical pulse is allowed to propagate through the segments using the Eq. (1.58). Firstly, the field $A(z,t)$ is propagated for a distance $h/2$, where the fiber non linearities are ignored and the dispersion term is taken into account. When the field $A(z,t)$ arrives at the middle part of the segment i.e. at $(z+\frac{h}{2})$, the effect of non linear term is involved. The propagation of the pulse for the remaining distance $\frac{h}{2}$ is governed by the inclusion of dispersive effects and finally $A(z+h,t)$ is obtained.

1.5.3. Far Field Power Spectrum

Let us take a laser pulse (Gaussian, Super Gaussian, Ultra short pulses etc) incident on a rectangular aperture at x-y plane. As the aperture is rectangular, let 2a be the width of the aperture along x-axis and 2b be the width along y-axis. The initial field of the incident field is given by [32].

$$E(x_{o,}y_o, z, t) = \exp\left(-\frac{x_o^2+y_o^2}{w_o^2}\right) A(t) \tag{1.60}$$

Where w_o is the beam waist, $A(t)$ is the temporal profile of the pulse of the form

$$A(t) = \exp\left(-\frac{(1+iC)t^2}{2T^2}\right) \exp(-i\omega_o t), \tag{1.61}$$

Where T is the pulse duration, C is the chirp parameter and ω_o is the central frequency of the pulse.

The initial incident field can be converted to frequency domain using the Fourier transforms. Thus the field in terms of frequency is given by:

$$E(x_{o,}y_o, 0, \omega) = \frac{1}{\sqrt{2\pi}} \int_{-\infty}^{\infty} E(x_{o,}y_o, 0, t) \exp(i\omega t)\, dt$$

$$= \exp\left(-\frac{x_o^2+y_o^2}{w_o^2}\right) F(\omega) \tag{1.62}$$

Where F $(\omega) = \frac{1}{\sqrt{2\pi}} \int_{-\infty}^{\infty} A(t) \exp(i\omega t)\, dt,$

depicts the Fourier Spectrum of the pulse at the incident plane and ω is the frequency.The initial power spectrum at the incident plane z=0 cane be obtained as In order to obtain the initial power spectrum, the Fourier spectrum is normalized as:

$$I_0(\omega) = |F(\omega)|^2 \tag{1.63}$$

To understand the wave propagation and to obtain far field spectrum, we use Huygens-Fresnel integration. The Eq. (1.62) satisfies Huygens-Fresnel integration and thus can be written as[33]:

$$E(x,y,z,\omega) = \frac{i}{\lambda z}\exp(-ikz)\iint_{-a-b}^{ab} E(x_o,y_o,0,\omega) \times \exp\left[-\frac{ik}{2z}\{(x-x_0)^2 + (y-y_0)^2\}\right] dx_o dy_o$$

where $k$is the wave number given by the expression $k = 2\pi/\lambda$.

Thus an analytical expression for far field power spectrum of a pulse can be obtained using Fourier Transformations. These far field approximations can be used to understand spectral switching.

Chapter-2

2.1 Elements of Spectral Switching and fiber optic sensors

Spectral switching is basically induced by diffraction. The zero intensity points found in the diffraction pattern are the phase singular points, where the spectral switching is observed. The essentials of spectral switching are discussed in this section. Also, since we aim to combine spectral switching effect in fiber optic sensors we briefly describe typical fiber optic sensors. The trick of combining spectral switching with sensors has wide scope. One can use nonlinear media/ nonlinear sensors to improve the system performance. Therefore, we also added the basic of nonlinear optics too.

2.1.1 Diffraction

Newton was of the view that light consists of a stream of particles. So Newton proposed the corpuscle theory of light according to which he believed that light is basically a form of particles. Yet his fellow, a Dutch physicist and astronomer Huygens said that light didn't consist of a stream of particles but he proposed the wave theory. His gave the idea that the light does not consist of stream of particles instead it travels by means of waves. Newton however challenged the wave theorist by saying that if light would have been a wave, then it should be able to bend around corners or diffract.

Later in 1660, an Italian physicist Francisco Grimaldi showed that a beam bent slightly outward after passing through a narrow aperture and named the phenomena as diffraction. The size of the aperture should be almost similar to the wavelength of the light used. In order to observe the diffraction pattern through a single slit, both the source and the observer should be far away from the obstructing surface, so the outgoing waves are parallel. The diffraction pattern can be obtained on the screen is diffraction pattern using a monochromatic light. The central part is bright and is generally larger than the dimensions of the slit. The

brighter band is bordered by alternate dark and bright bands with rapidly decreasing intensity. The phenomena of diffraction and the pattern obtained by diffraction through circular aperture are shown in the Fig. (2.1)(a) and (b).

Each point on the wave front acts as the source of secondary wavelets. This is basically the Huygens principle. The wave fronts are perpendicular to the waves. The combined effect of these wavelets results in the bright or dark fringe. The correct explanation in terms of wave theory, we owe to the brilliant work of Fresnel.

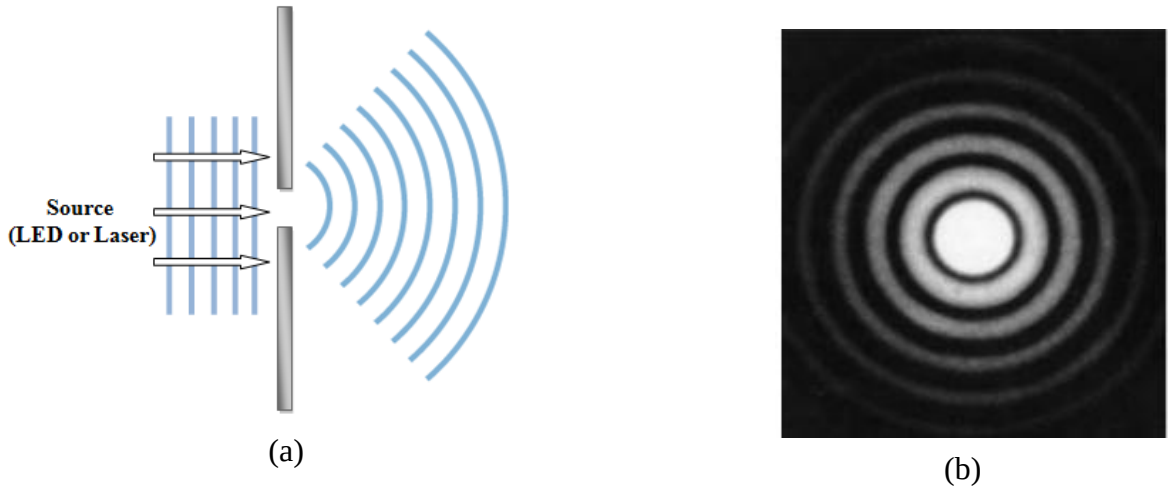

(a) (b)

Figure 2.1 (a) The phenomena of diffraction from a single slit. (b) the diffraction pattern from a circular aperture[Image courtesy: http://www.goldastro.com/goldfocus/diffraction_theory.php].

According to Fresnel, in regions well beyond the regions of geometrical shadow, the secondary wavelets arrived with phase relations such that they interfere destructively and produce practically complete darkness. In Fresnel diffraction, we actually divide the aperture into regions called Fresnel Zones. As the screen is moved away from source up to some finite distance and the wave fronts are cylindrical and spherical. This is known as Fresnel Diffraction. On the other hand, in Fraunhofer diffraction, the source and the screen are at infinite distance from the obstacle and the wave front is called plane wave front.

2.1.2 Spectral Switching

Spectral Switching is one of the phenomena observed in the domain of singular optics. We generally observe two types of spectral switching depending upon the variation in diffraction angle.

2.1.2.1 On axis spectral shift- In this case the spectrum is initially symmetrically distributed around the central frequency whereas after passing through the aperture, diffraction takes place and the spectrum is shifted towards the higher frequency region i.e. towards the frequency of blue light. As the spectrum shifts towards the higher frequency region and blue color has the highest frequency, this phenomenon is referred as Blue shift [34]. Fig (2.2) illustrates the on-axis shift of the spectrum towards the higher frequency region.

2.1.2.2 Off axis spectral shift-At a certain value of diffraction angle, the spectrum is divided into two peaks of equal height, this angle is known as critical angle. At an angle smaller than this critical angle, the spectrum shifts towards the lower frequency region i.e. the spectrum is Red shifted. Again as the spectrum is shifted towards the lower frequency region and red color has the lowest frequency, hence the shift is called red shift [34]. Fig (2.3) shows the blue-shift and the red-shift of the central frequency and the critical angle.

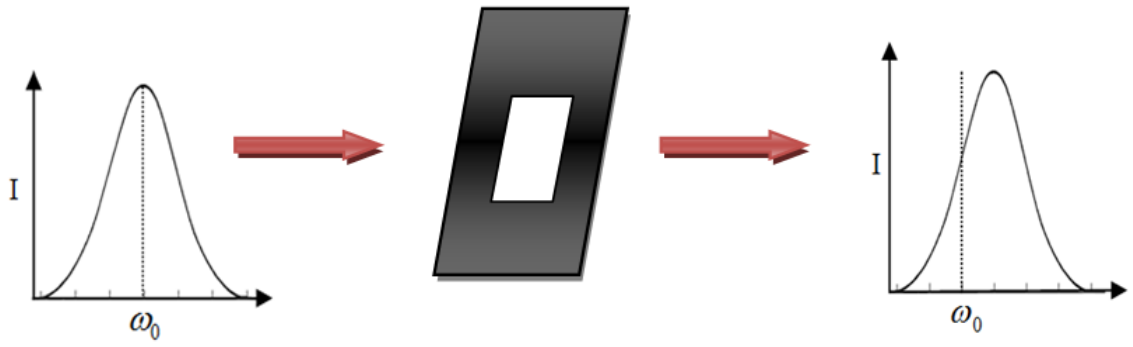

Figure 2.2 The on-axis blue shift.

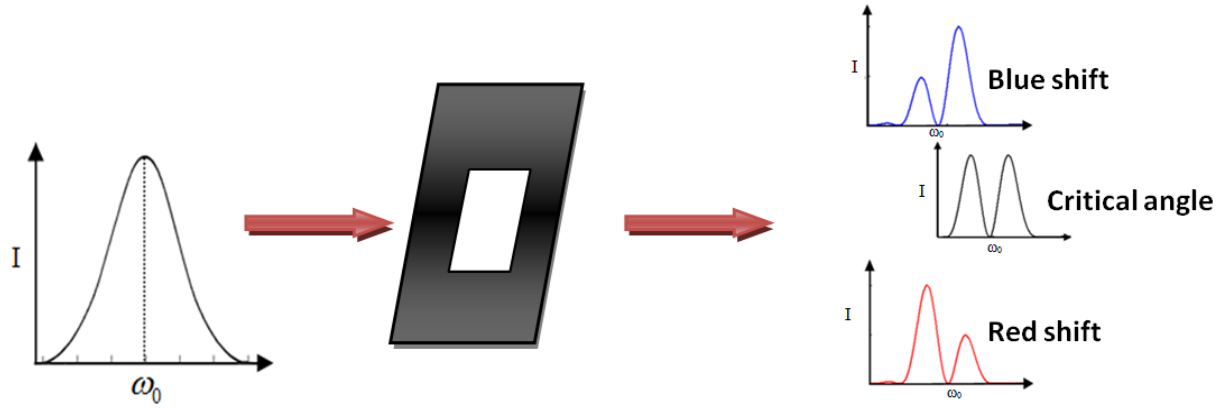

Figure 2.3 The off-axis spectral switching showing the critical angle at which peak is divided into equal parts.

2.1.3 Nonlinear Optics

The laser was invented in 1960 and one year afterwards in 1961, the high intensities obtained from the lasers opened up the new field of optics where the interaction between the light and the material in which it propagated was no longer described by the simple form of the Maxwell equations but by an extended form including a non linear response. The initial trigger in 1961 got everyone excited about the field of nonlinear science and optical frequencies. After a while it was believed that all the simple as well as complex phenomena can be explained by nonlinear optics. Basically, nonlinear optics is the branch of optics that deals with the behavior of light in nonlinear media i.e. media in which the dielectric polarization P responds in a non-linear manner to the electric field E of the light. The linear and the non linear dependence of the polarization P on the electric field E is shown in the Fig. (2.4). This nonlinearity is typically only observed at very high intensities such as those provided by lasers. The superposition principle does not hold in the nonlinear optics. Many new phenomena like creation of new frequency or modulation in phase and shape of the beam or the pulse occur due to this nonlinear response.

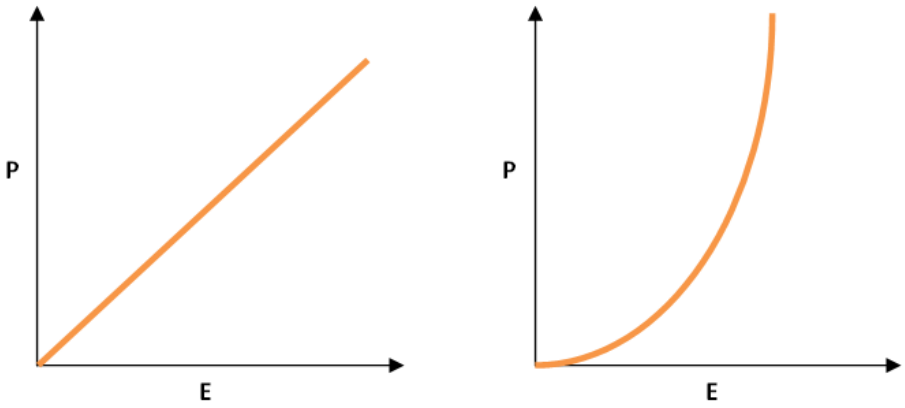

Figure 2.4 The linear and non linear dependence of Polarization P on the electric field E.

Normal light is not suitable for studying nonlinear optics because it is weak as compared to the highly intense light which has the strength to change the properties of the light. Thus the invention of laser promised a new platform to uplift the branch of nonlinear optics. Peter Franken and his fellows demonstrated the generation of new photons with twice the frequency of the initial photons in using highly intense laser in 1961 at the University of Michigan (USA). It is generally said to be the generation of second harmonic of light. Further in 1962, the third harmonic generation of light was investigated which is also called frequency-tripling. The period of 1961-1963 laid the basic foundation for further evolution of nonlinear optics. These influential developments lead to the explosion of study in the domain of studying nonlinear effects like stimulated Raman or Brillouin scattering, four wave mixing, stimulated Rayleigh scattering and many more such phenomena. In general the number of nonlinear optical phenomena exceeds the linear optical phenomena due to the significant and valuable results of the former. The nonlinear optical phenomena are observed at high intensities. Thus after the invention of laser, this branch faced a revolutionary uplift.. Though the linear phenomena are relatively easier, yet nonlinear phenomena are more in number as compared to the linear phenomena. The reason behind this lies in the fact that many of the phenomena can't be understood with linear optics; however nonlinear optics provides a better platform for studying those complex phenomena. The generation of second harmonic of light, also called frequency doubling, leads to the generation of

two photons i.e. the frequency is doubled. As the frequency depends on energy, this implies that the energy is doubled and the energy remains conserved. This observation can open new pathways to produce more energy from single photons.

Moreover, the areas in which linear optics cannot venture, nonlinear optics play an important role. Linear optics can't be used to make soliton whereas non linear optics has the capability to produce a quantized structure called soliton. This quantized structure has a large ability to pass data information. Thus nonlinear optics can be used for optical communication, optical switching, optical data-processing etc. Also the nonlinear optics can be used to study the physical properties of the materials using spectroscopy. The concept of nonlinear optics is triggering the advancement in many other novel areas. The formation of optical circuits has provided a new facet to enhance the speed of computing and networking than the electronic gadgets. Optical amplifiers with minimum loss can be used to transmit data up to thousands of kilometers. Thus nonlinear optics has promised a new era of optical communication by providing endless paths for research.

2.1.4 Fiber Optic Sensors

From the name it is clear that fiber optic is composed of two words, fiber which is a very thin glass object and optics means light. So, fiber optics means light that travels in some glass or plastic fibers where a bunch of fibers are surrounded by a strong jacket around them. The glass fiber is composed of three layers. There is a core at the centre which has a higher refractive index. The outer portion of the core comprises of the cladding layer which has comparative lower refractive index. The third layer is the plastic buffer coating. This layer does not perturb the performance of optical fiber. It simply provides the mechanical protection to the inner parts of the fiber. The core and the cladding layers are all based on the fused silica which is a fiber glass. But this fused silica is extremely clear with almost no impurities. Fig. (2.5)(b) shows the structure of an optical fiber with core and cladding. This transparency is extremely important so that the light can travel for a very long distance such as hundreds kilometers with minimum loss and this makes the fiber optic communication possible.

Here comes the question that why the light doesn't gets leaked out of the fiber. The principle of propagation of light in an optical fiber is based upon the total internal reflection. The phenomenon of total internal reflection in an optical fiber is shown in Fig. (2.5)(a). Due to this reason the light is transmitted through an optical fiber. Snell's law guides that how light travels at the interface of core and cladding. When the light is incident at the interface between the core and cladding at different angles, some of its power is reflected back and some of the power enters into the cladding which is refracted. When we increase the incident angle to the value greater than the critical angle θ_c, no light enters the cladding. All light is reflected back to the core. This is the phenomenon of Total Internal Reflection. The important point to be considered here is θ_c, i.e. if light enters the fiber less than θ_c, it will quickly leak out of the fiber and won't travel long. When the light enters the fiber at an angle greater than θ_c, it will be bounced back and forth at the interface of core and cladding and it will travel a long distance with minimum loss.

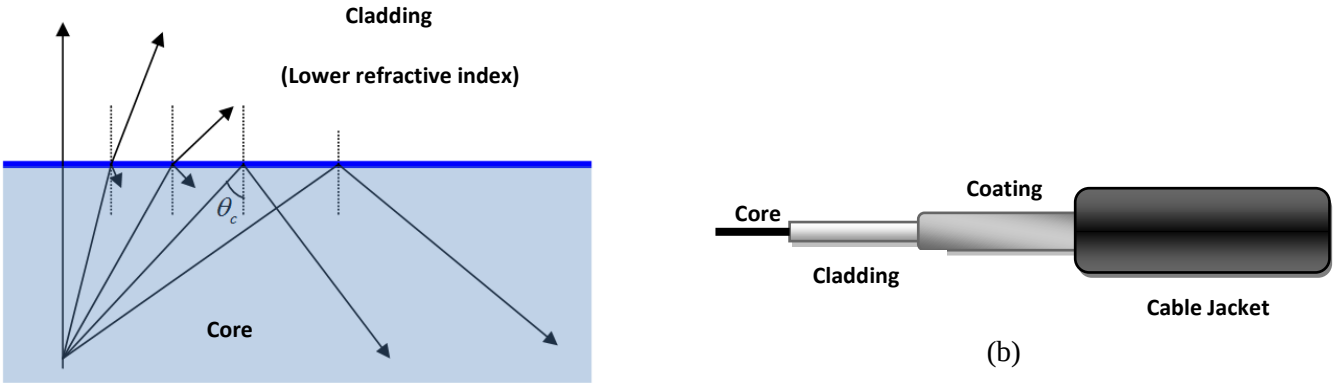

Figure 2.5 (a) The phenomenon of total internal reflection taking place at the interface of core and cladding. (b) structure of an optical fiber.

A sensor is a device which converts any physical phenomena into an electrical quantity essentially. A transducer converts any such phenomena into other physical phenomena which cannot be generally electrical. Now in the fiber optic sensing system, fiber acts as the sensing element. The light from the optical source is transmitted to the sensor along the optical fiber. The sensor gets affected by the changes in the desired environmental parameter. Due to this, the sensor further modulates the characteristics of the light (Intensity, phase, polarization

etc.). The modulated light is then passed on to the detector which detects the modulation of the above parameters and thus the effect of perturbation in certain parameters of the environment can be detected in terms of the modulated light. The fiber optic sensors can be classified into two types based on their structures: Intrinsic and Extrinsic as shown in the Fig. (2.6). In Intrinsic FOS (Fiber Optic Sensor), the fiber acts as the sensing element. Due to the affect of external properties, the light passing through the intrinsic fiber gets modulated. In extrinsic FOS, the fiber simply behaves as the transporter. The light is passed into the some other optical sensing element through fibers and then again modulated light is received through the fiber.

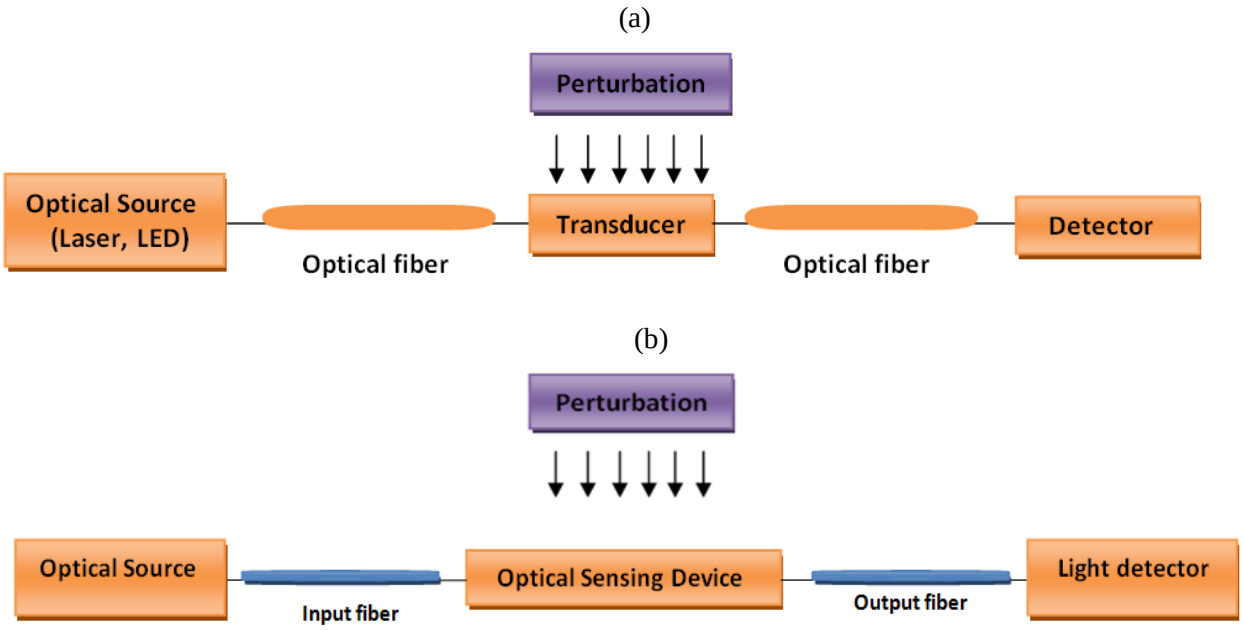

Figure 2.6 Schematic diagrams of (a) Intrinsic fiber optic sensors. (b)Extrinsic Fiber optic sensors.

Fiber optic sensors have proved out to be a boon in disguise. Their enhanced use has fueled the demand of optical fibers. They have the following applications over other detectors:

- provide an efficient transmission with minimum loss,
- the information is secured as there is no loss of data outside the cladding,
- no sparkling and thus avoids the risk of fire hazards,

- resistant to hazardous environments,
- due to small size and light weight, can be used at even those places where it becomes difficult to implant any wire system,
- Immune to interference by some outside signals.

Chapter-3

3.1 Results and Discussion

3.1.1 Improvement in response of fiber optic pH sensor by using spectral switching

Chemical and biochemical sensors have proved out to be a milestone in the advancement of sensor technology. The pH sensors have emerged among significant optical tools used in industrial, agricultural and biological areas. [35] We are using the concept of pH fiber optic sensors using sol-gel films. The various indicators are used to detect the change in the pH in the surroundings. The pH indicators are immobilized by sol-gel films. The various indicators used are thymol blue, cresol red and BTB (bromthymol blue). The light enters into the pH sol gel film embedded in the pH sensing probe through optical fibers. The pH sensing probe detects the change in the pH and thus the change in color of the sol-gel films indicates the corresponding change in pH. This change is reflected in the optical characteristics of the light. The modulation in the optical properties helps in the diagnosis of the amount of change in pH in the surroundings [36].

As an extension to the concept of developing fiber optic pH sensors using sol-gel films [36], we have introduced the spectral switching phenomenon along with the sensors. From the graph reporting how the wavelength varies with intensity when the value of pH is changed (see Appendix A), we can calculate the Full Width Half Maximum (FWHM). Three different materials are used as indicators to detect the various values of pH. Using FWHM we found the different values of delta (δ) where δ is the truncation parameter. The variation of FWHM and pH is shown in the Fig. 3.1 (a), (b) and (c).

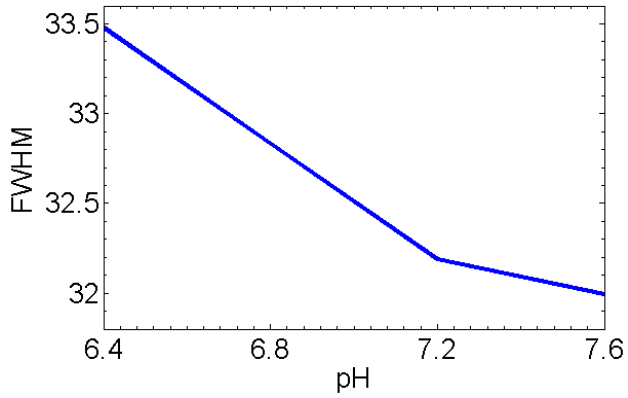

Figure 3.1(a) The variation of FWHM with pH using BTB based sol-gel film.

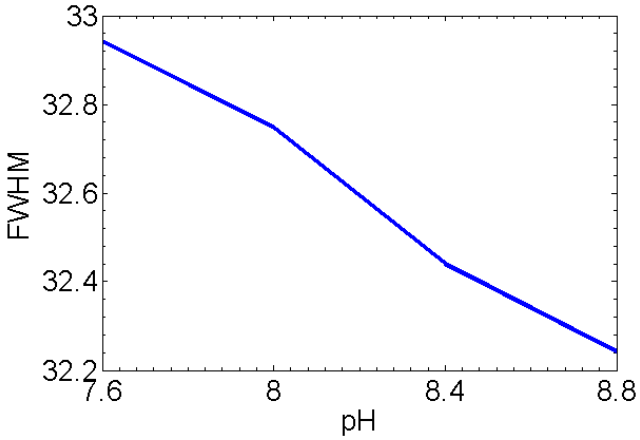

Figure 3.1(b) The variation of FWHM with pH using cresol-red based sol-gel film

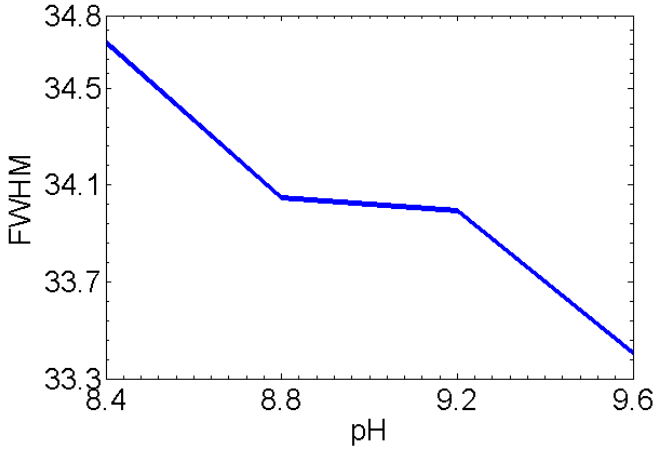

Figure 3.1(c) The variation of FWHM with pH using Thymol-blue based sol-gel film.

Using the fixed normalized aperture size equal to 26, we can compute delta (δ) which is the ratio of aperture size to the calculated FWHM. Thus the value of δ has been found. Now we can find the pH vs. delta (δ) curve as shown in Fig. 3.2 (a), (b) and (c). It is seen that δ increases with the increase in the value of pH even if different materials are used as an indicator.

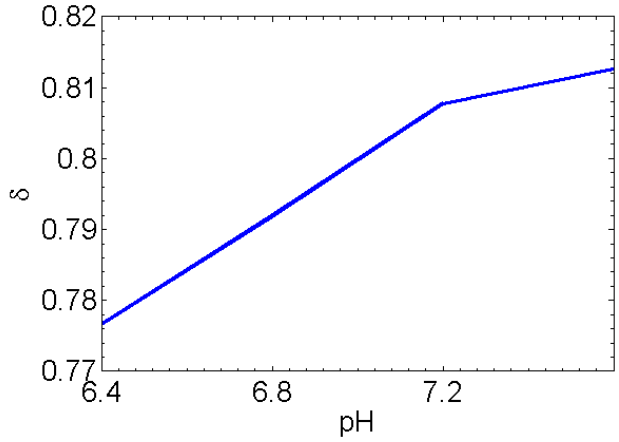

Figure 3.2(a) The variation of delta (δ) *with pH using BTB based sol-gel film.*

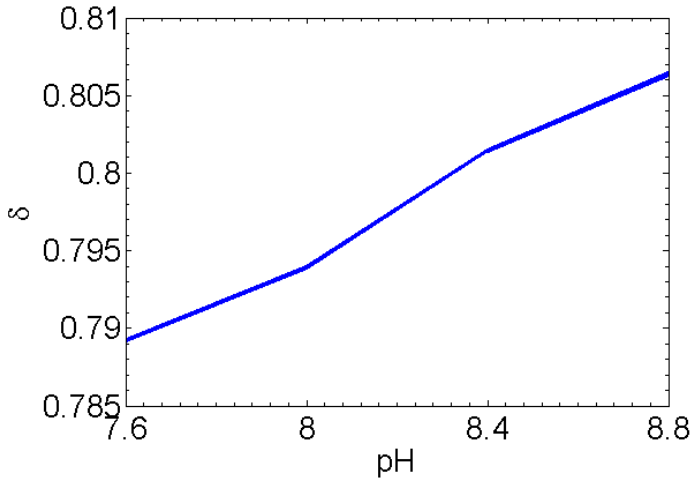

*Figure 3.2(b) The variation of delta (*δ*) with pH using cresol-red based sol-gel film.*

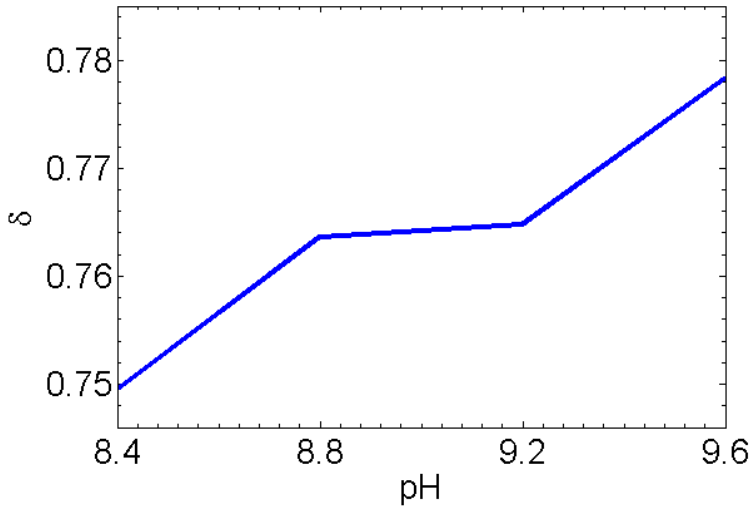

Figure 3.2(c) The variation of delta (δ) with pH using Thymol-blue based sol-gel film.

We basically need to emphasize upon the dependence of critical angle on pH because the value of critical angle is important for determining the switching phenomena. At this angle the peak is divided into two equal parts. Above (below) this angle, blue (red) shift takes place. Fig. 3.3 (a), (b) and (c) shows the variation of critical angle (α) for the values of delta (δ).

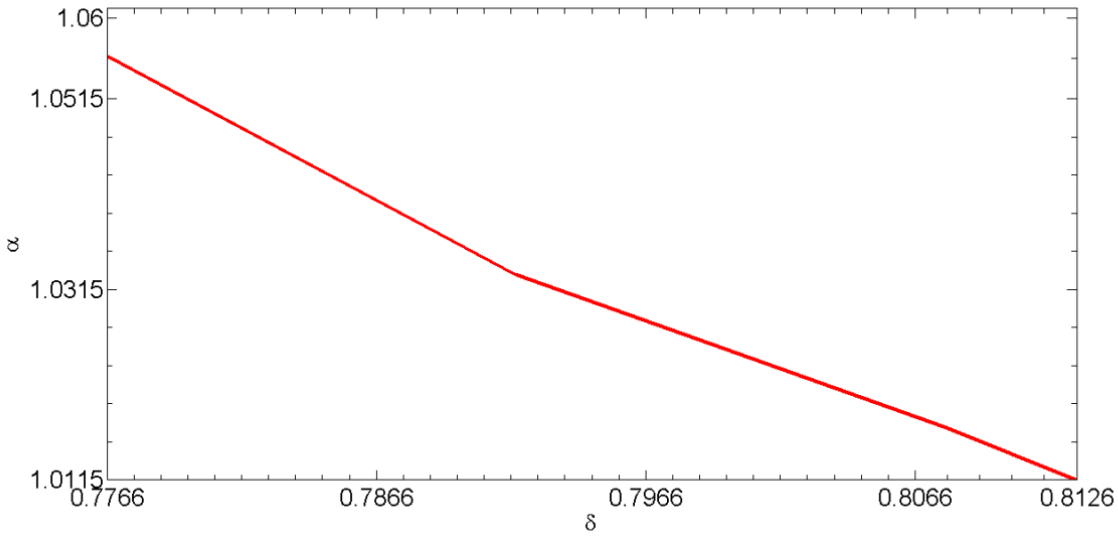

Figure 3.3(a) The variation of α with δ using BTB based sol-gel film.

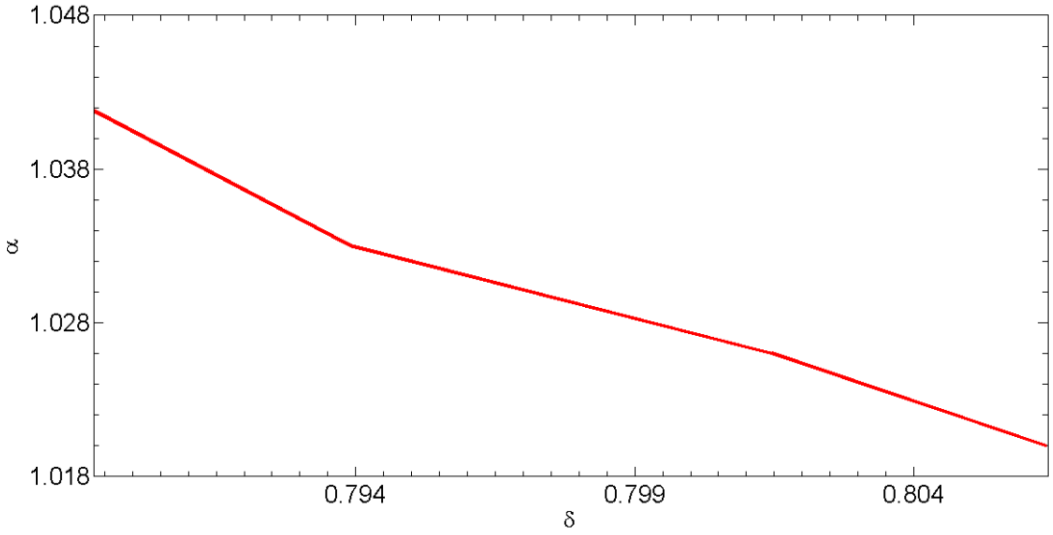

Figure 3.3(b) The variation of α with δ using cresol-red based sol-gel film.

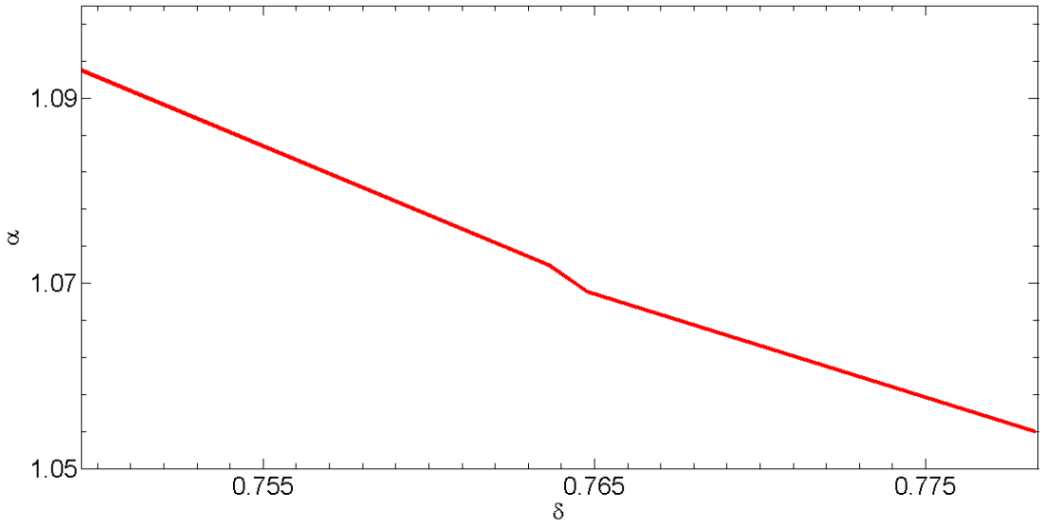

Figure 3.3(c) The variation of α with δ using Thymol-blue based sol-gel film.

Fig. 3.3 (a), (b) and (c) confirms that switching occurs at lower critical angles as the value of delta (δ) is increased. Our main motive is to find the variation of pH with the critical angle (α). Combining the results of Fig. 3.2 and Fig.3.3 we finally get the variation of critical angle of switching with pH. This is shown in Fig. 3.4. This result is of great significance because the effect of changing pH has altered the values of critical angles. For various indicators and

increasing value of pH, the critical angle (α) decreases. The dependency of pH on critical angle shows that critical switching occurs at lower angles for higher values of pH.

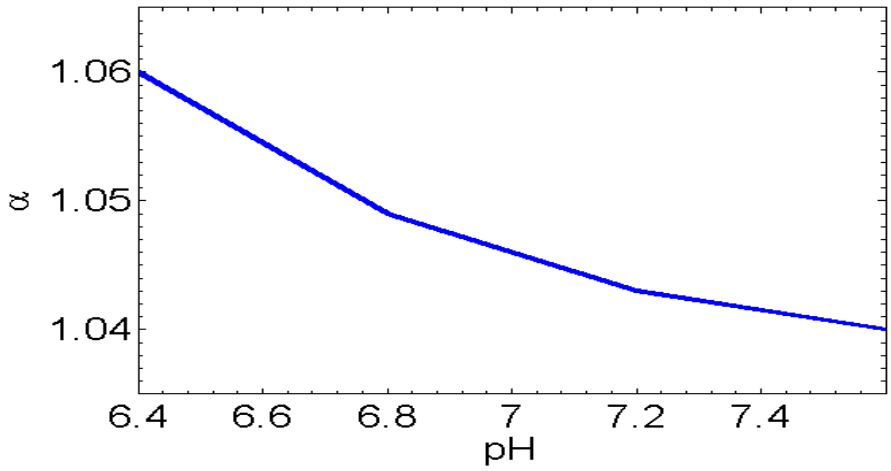

Figure3.4(a) The variation of α with pH using BTB based sol-gel film.

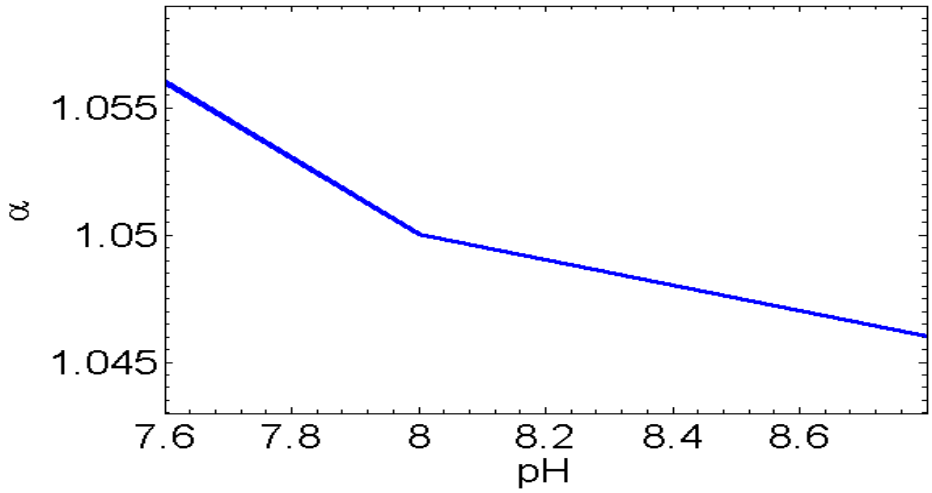

Figure 3.4(b) The variation of α with pH using cresol-red based sol-gel film.

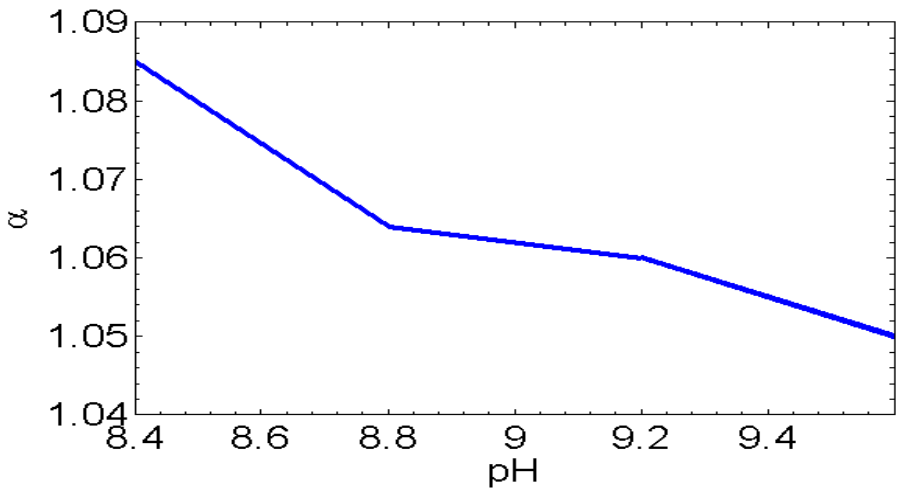

Figure 3.4(c) The variation of α with pH using Thymol-blue based sol-gel film.

3.1.2 Improvement in response of fiber optic relative humidity sensor by using spectral switching

Relative Humidity is the amount of water as a vapor present in the air compared to the maximum amount of vapor it can contain. The more the air temperature is, more the moisture it can retain. As the temperature is increased, the number of vapors increases in the air. The study of relative humidity is of major importance to the meteorological as well as agricultural department. A humidity sensor is generally referred to as hygrometer. It senses and determines the amount of humidity existing in the air. It therefore measures both temperature and moisture present in the air.

But these sensors are not efficient in harsh environments and due to their low response time, accurate results cannot be obtained. So, fiber optic humidity sensors have gained much importance in this field due to their remarkable properties. Since now, cobalt chloride, phenol red and crystal violet have been used as the sensing materials because they are more sensitive to humidity. Hygroscopic polymer sensors are generally used to detect the humidity variations because these polymers expand after absorbing moisture from the air. The expansion of the

polymer leads to a change in the refractive index of the coating and further leading to the change in the properties of light passing through. The Thin Core Fiber Modal Interferometer (TCFMI) is introduced to measure the change in refractive index due to the volume expansion of polymers. The FBG (Fiber Bragg Grating) nullifies the measurements arising due to interference of temperature. This type of fiber optic sensor was then used to measure the spectral response of the sensor by varying the values of relative humidity at various temperatures. It was observed that the transmission dip shifts to the longer values of wavelength as the %RH increases [37].

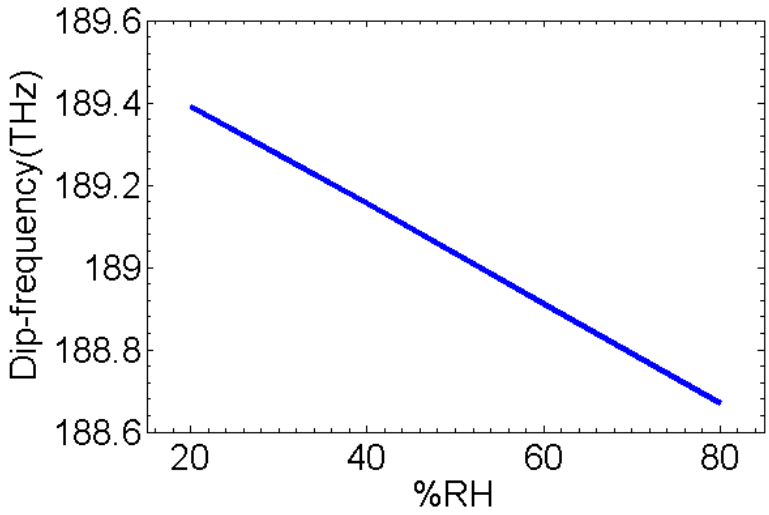

Figure 3.5 The dip frequency shifts to lower values as the %RH increases.

Fig (3.5) shows the response of sensor to the increase in %RH in terms of frequency. The transmission dip shifts to shorter frequencies as the %RH increases. Fig. (3.6) shows the transmission spectra illustrating the dip frequency moves towards lower values of frequency as the relative humidity increases [37]. Here the values of %RH are considered in the increasing order as 20%, 30%, 40%, 60% and 80%.

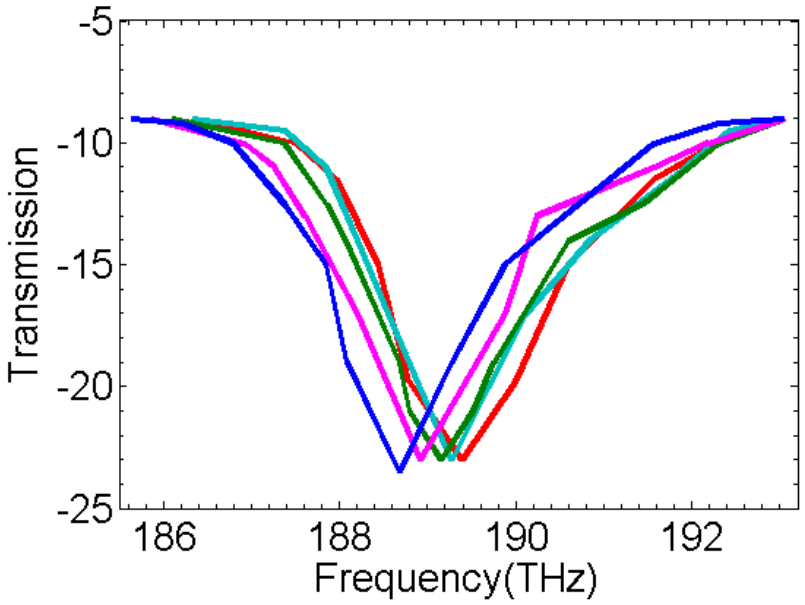

Figure 3.6 Transmission spectra for different relative humidity without spectral switching. The dip frequency shifts with the relative humidity.

Now by using an aperture in front of the sensors merged with fiber modal interferometer, the values of frequency will include a shift arising due to spectral switching. The first dip frequency occurs at 189.39THz. The on-axis blue shift (see Appendix B) shifts the normalized central frequency by 0.25. This shift is calculated without using sensor. Using the normalized value of shift (0.25) and computing this value with the frequency shift due to increment in %RH, the dip frequency shifts to 194.124 THz. This is shown in the Fig. (3.6).

Table-1 shows the increase in the dip frequency with increment in relative humidity. It is clear from the table that after including the spectral switching, the dip frequency shifts significantly to higher values.

TABLE-1

Different values of dip frequency varying with increase in humidity.

Relative humidity (%)	Dip-Frequency Without spectral switching (THz)	Dip-Frequency With spectral switching (THz)
20	189.39	194.274
30	189.274	194.0058
40	189.155	193.8838
60	188.91	193.6247
80	188.67	19.3867

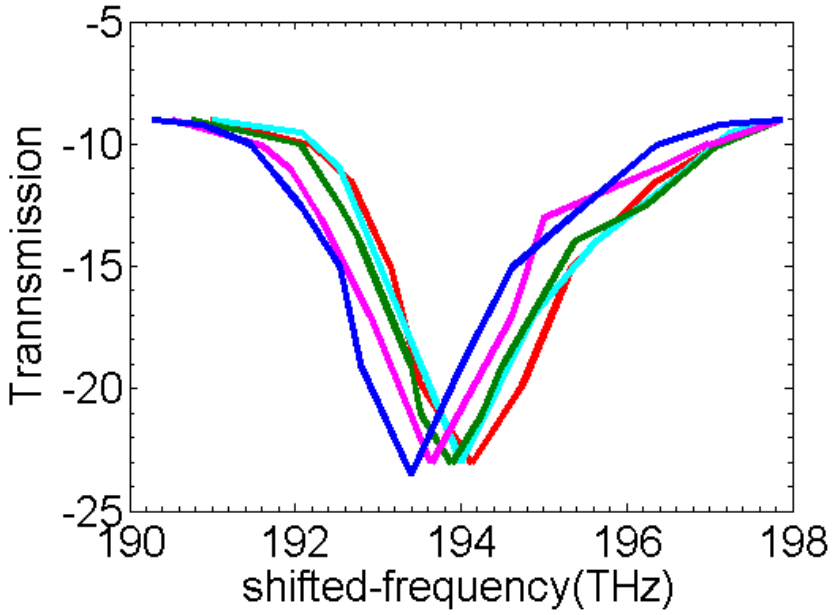

Figure 3.7 Transmission spectra for different relative humidity in presence of spectral switching. The dip frequency shifts with the relative humidity. This shift is greater than that of Fig.3.6.

Table-2 shows the difference in dip frequency for increase in %RH. It can be clearly seen from the table that the difference increases significantly in terms of Terahertz. Thus the combination of spectral switching with fiber optic relative humidity sensor will increase the sensitivity of the sensor remarkably.

TABLE-2

Difference in dip frequency with and without spectral switching

Relative humidity (%)	Difference in Dip-Frequency Without spectral switching (THz)	Difference in Dip-Frequency With spectral switching (THz)
20-30%	0.24	0.246
20-40%	0.485	0.4971
20-60%	0.604	0.6191
20-80%	0.72	0.7373

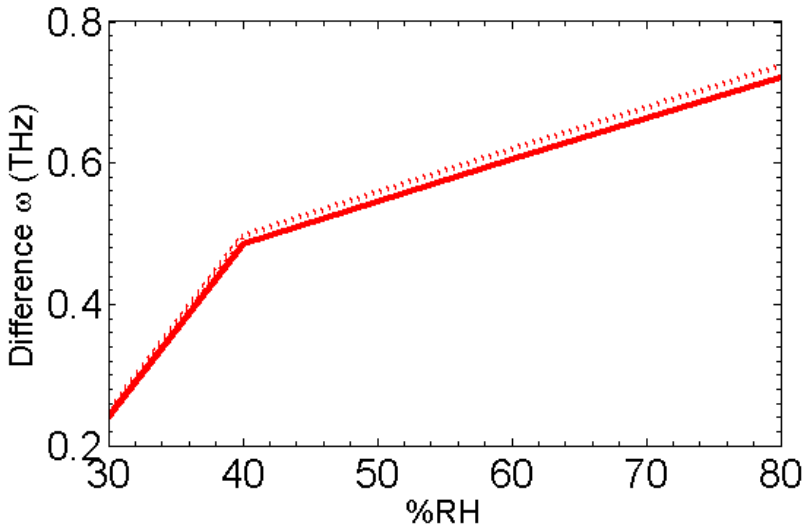

Figure 3.8 Difference in the dip frequency for different % relative humidity without (solid line) and with (dotted line) spectral switching.

Here the difference increase significantly in terms of Tera-Hertz, this will increase the sensitivity of the sensor towards the environmental effects. Such a better level of sensitivity will help to investigate the humidity effects more accurately. Thus the results can be calculated more efficiently by combining the spectral switching and fiber optic sensor technology.

3.2 Conclusion

We investigated the performance of fiber optic pH sensor and relative humidity sensor by combining them with aperture that creates diffraction induced spectral switching. The variation of critical angle with pH has been observed. Our investigation shows that the critical angle decreases with increase in pH using different materials as indicators. This variation is of great significance as the results of spectral switching are influenced by the change in pH of the surroundings. This can increase the sensitivity of the sensor towards the environment.

Further the effect of spectral switching has been introduced to relative humidity sensor. In this case too the performance of the sensor improves drastically. The effect of relative humidity (RH) on the central frequency has been discussed. The effect of relative humidity leads to the shifting of dip frequency to higher values. However when the normalized vale of the shift is analyzed along with this shift of frequency due to RH, it is observed that the actual value shifts by a large amount. This outcome has a great implication because the change is quite significant i.e. in terms of Terahertz. The result can help to increase the sensitivity of the sensors. Also it is helpful for distant optical communication or space communication. It can also provide better optical switching and data coding-decoding mechanism with enhanced sensitivity and can be utilized even in harsh environments.

List of figures

Figure 1.1 (a) The image showing the working of fiber optic sensors (b) the collaboration of fiber optic sensors and spectral switching as sensors. 5

Figure 2.1 (a) The phenomena of diffraction from a single slit (b) the diffraction pattern from a circular aperture. 21

Figure 2.2 The on-axis blue shift. 22

Figure 2.3 The off-axis spectral switching showing the critical angle at which peak is divided into equal parts. 23

Figure 2.4 The linear and non linear dependence of Polarization P on the electric field E. 24

Figure 2.5 (a) The phenomenon of total internal reflection taking place at the interface of core and cladding**.** (b) structure of an optical fiber. 26

Figure 2.6 Schematic diagrams of (a) Intrinsic fiber optic sensors. (b) Extrinsic Fiber optic sensors. 27

Figure 3.1(a) The variation of FWHM with pH using BTB based sol-gel film. 30

Figure 3.1(b) The variation of FWHM with pH using cresol-red based sol-gel film 30

Figure 3.1(c) The variation of FWHM with pH using Thymol-blue based sol-gel film. 30

Figure 3.2(a) The variation of delta with pH using BTB based sol-gel film. 31

Figure 3.2(b) The variation of delta with pH using cresol-red based sol-gel film. 31

Figure 3.2(c) The variation of delta with pH using Thymol-blue based sol-gel film. 32

Figure 3.3(a) The variation of alpha with delta using BTB based sol-gel film. 32

Figure 3.3(b) The variation of alpha with delta using cresol-red based sol-gel film. 33

Figure 3.3(c) The variation of alpha with delta using Thymol-blue based sol-gel film. 33

Figure 3.4(a) The variation of alpha with pH using BTB based sol-gel film. 34

Figure 3.4(b) The variation of alpha with pH using cresol-red based sol-gel film. 34

Figure 3.4(c) The variation of alpha with pH using Thymol-blue based sol-gel film. 35

Figure 3.5 The dip frequency shifts to lower values as the %RH increases. 36

Figure 3.6 The dip frequency shifts towards the higher values as the relative humidity increases. 37

Figure 3.7 The dip frequency further shifts towards higher values by including the effect of aperture. 38

Figure 3.8 The difference in actual frequency and the shifted frequency due to effect of aperture. 39

References

1. M. S. Soskin and M. V. Vasnetsov, Progress in Optics, Ed. E. Wolf, (Elsevier,2001)42, 219.
2. M. S. Soskin and M. V. Vasnetsov, Pure Appl. Opt. 7, (1998) 301-311
3. J. F. Nye and M. V. Berry, Proc. R. Soc. London A 336, (1974)165.
4. G Gbur, T. D. Visser and E. Wolf, Phys. Rev. Lett., 88, (2002) 013901.
5. G Gbur, T. D. Visser and E. Wolf, J. Opt. Soc. Am A, 19, (2002) 1694.
6. M. V. Berry, New J. Phys 4 (2002) 66.
7. H. C. Kandpal, J. Opt. A: Pure Appl. Opt., 3 (2001) 296 and H. C. Kandpal, S. Anand and J. S. Vashya, IEEE J. Quantum Elec., 38(2002) 336].
8. D. A. Kessler and I. Freund, Opt. Lett., 28 (2003) 111
9. C. Palma and G. Cincotti , J. Opt. Soc. Am A, 14, (1997) 1885 and C. Palma and G. Cincotti , Opt. Lett., 22 (1997) 671
10. Bai-da Lu and Liu-Zhan Pan,IEEE J. Quantum Electron., 38 (2002) 340
11. Jixiong Pu and Shojiro Nemoto,IEEE J. Quantum Electron, 36(2000) 1407
12. Liu-Zhan Pan and Bai-da Lu, IEEE J. Quantum Electron., 39 (2003)1334
13. G. Zhao, X. Xiao and B. Lu, Chin. Phys., 13 (2004) 2064
14. L. Pan and B. Lu, IEEE J. Quantum Electron., 37 (2001)1377 and J.Pu and C.Cai, Chin. Phys. Lett., 21 (2004) 1268.
15. H. Hwang , G Yang and P Han, Opt. Eng. 42 (2003) 686
16. Liu-Zhan Pan and Bai-da Lu, Chinese Physics, 13 (2004) 637 and Liu-Zhan Pan and Bai-da Lu, Optik, 115 (2004) 57
17. S. Jana, S.Konar, Optics Communication 267(2006) 24-51.
18. H.C. Kandpal, Optics Communications 277 (2007) 24–32.
19. P.Diament, Wave Transmission and Fiber Optics (Macmillan, New York, 1990), Chap 3.
20. N. Bloembergen, Nonlinear Optics (Benjamin, Reading, MA, 1977), Chap 1.
21. Y.R. Shen, Principles of Nonlinear Optics (Wiley, New York, 1984).
22. P. N. Butcher and D. N. Cotter, *The Elements of Nonlinear Optics* (Cambridge University Press, Cambridge, UK, 1990).

23. R. W. Boyd, *Nonlinear Optics*, 2nd ed. (Academic Press, Boston, 2003).
24. Y. R. Shen, *Principles of Nonlinear Optics* (Wiley, New York, 1984), Chap. 1.
25. M. Schubert and B. Wilhelmi, *Nonlinear Optics and Quantum Electronics* (Wiley, New York, 1986), Chap. 1.
26. P. N. Butcher and D. N. Cotter, *The Elements of Nonlinear Optics* (Cambridge University Press, Cambridge, UK, 1990), Chap. 2.
27. G. P. Agrawal, in *Supercontinuum Laser Source*, R. R. Alfano, ed. (Springer-Verlag, Heidelberg, 1989), Chap. 3.
28. H. A. Haus, *Waves and Fields in Optoelectronics* (Prentice-Hall, Englewood Cliffs, 1984), Chap. 10.
29. P. M. Morse and H. Feshbach, *Methods of Theoretical Physics* (McGraw-Hill, New York, 1953), Chap. 9.
30. J. A. Fleck, J. R. Morris, and M. D. Feit, *Appl. Phys.* 10, 129 (1976).
31. M. Lax, J. H. Batteh, and G. P. Agrawal, *J. Appl. Phys.* 52, 109 (1981).
32. Soumendu Jana, S.Konar, Optics Communication 267(2006) 24-51.
33. Liu-Zhan Pan, Bai-da Lu, Optik 115(2004) 57.
34. S. Jana, S.Konar, Optics Communication 267(2006) 24-51.
35. Jie lin, In Recent development and Applications of Optical and Fiber Optic pH-sensors (Trends in analytical chemistry, vol. 19, no. 9, 2000).
36. Wook Jae Yoo, Jeong Ki Seo et.al (2011). *Development of Reflection-type Fiber-optic pH Sensor Using Sol-gel Film* (Journal of Sensor Science and Technology) Vol. 20, No. 4 (2011) pp. 266-271.
37. Bobo Gu1, Ming-Jie Yin et.al (2009). *Low-cost high-performance fiber-optic pH sensor based on thin-core fiber modal interferometer*. Vol. 17, No. 25 / Optics Express 22302

Appendix A

The intensity variation of the peak wavelength has been shown, when different materials are used as indicators.

[Wook Jae Yoo, Jeong Ki Seo et.al (2011). *Development of Reflection-type Fiber-optic pH Sensor Using Sol-gel Film* (Journal of Sensor Science and Technology) Vol. 20, No. 4 (2011) pp. 266-271]

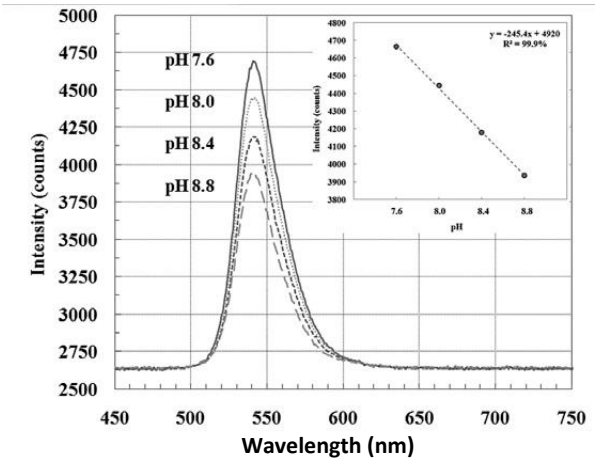

Fig-(3.9) Intensity variation of the peak wavelength when cresol red-based sol-gel film is used.

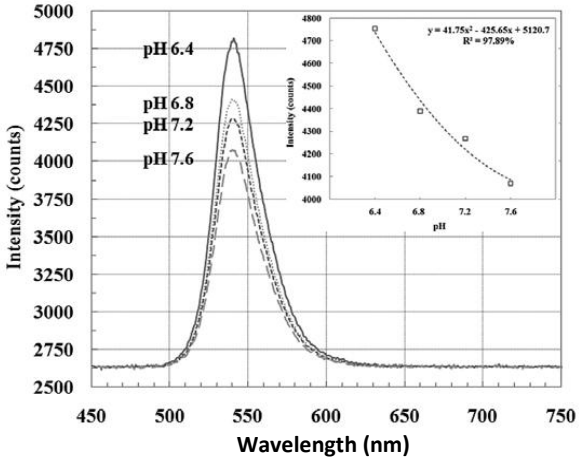

Fig-(3.10) Intensity variation of the peak wavelength when BTB-based sol-gel film is used.

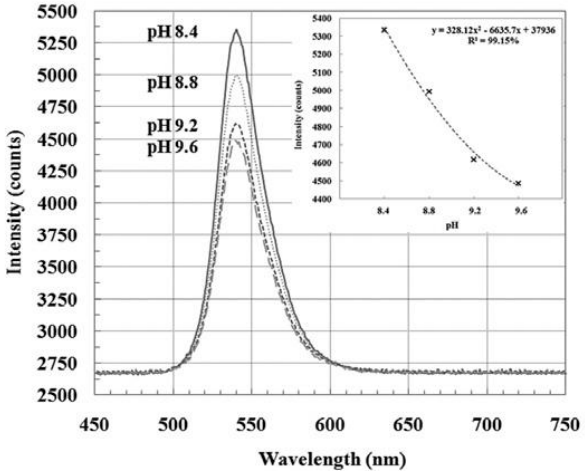

Fig-(3.11) Intensity variation of the peak wavelength when thymol-blue based sol-gel film is used.

Appendix B

The initial spectrum is symmetrically distributed around the central frequency whereas the far-field spectrum is shifted towards higher frequency region i.e. towards the frequency of blue light. The normalized shift when calculated comes out to be 0.25.

[Soumendu Jana, S.Konar, *Tunable spectral switching in the far field with a chirped cosh-Gaussian pulse*, Optics Communication 267(2006) 24-51.

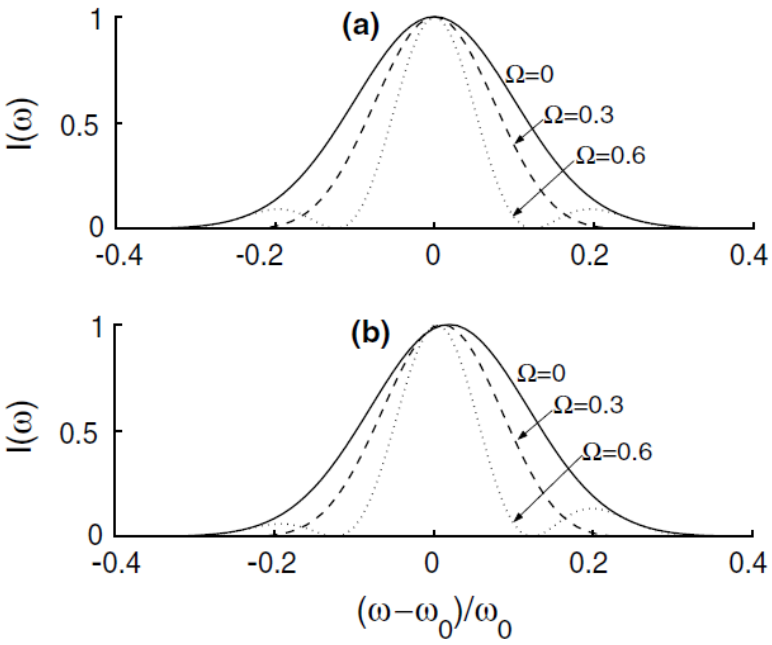

Figure 3.12 (a) Normalised near field on-axis power spectrum. (b) modified far field spectrum